Available online at www.sciencedirect.com

SciVerse ScienceDirect

journal homepage: www.JournalofSurgicalResearch.com

Thyroid stimulating hormone increases iodine uptake by thyroid cancer cells during BRAF silencing

David A. Kleiman, MD,[a,1] Daniel Buitrago, MD,[a,1] Michael J. Crowley, BS,[a] Toni Beninato, MD,[a] Alexander J. Veach, BS,[b] Pat B. Zanzonico, PhD,[b] Moonsoo Jin, DSc,[c] Thomas J. Fahey III, MD,[a] and Rasa Zarnegar, MD[a,*]

[a] Division of Endocrine and Minimally Invasive Surgery, Department of Surgery, New York Presbyterian Hospital-Weill Cornell Medical College, New York, New York

[b] Department of Radiology and Program in Molecular Pharmacology and Chemistry, Memorial Sloan Kettering Cancer Center, New York, New York

[c] Department of Biomedical Engineering, Cornell University, Ithaca, New York

ARTICLE INFO

Article history:
Received 8 June 2012
Received in revised form
21 July 2012
Accepted 24 August 2012
Available online 8 September 2012

Keywords:
Papillary thyroid cancer
BRAF (V600E) mutation
Radioactive iodine
Radioactive iodine resistance
Thyroid-stimulating hormone
Sodium–iodine symporter

ABSTRACT

Background: The $BRAF^{V600E}$ mutation is present in 62% of radioactive iodine–resistant thyroid tumors and is associated with downregulation of the sodium–iodide symporter (NIS) and thyroid stimulating hormone receptor (TSHr). We sought to evaluate the combined effect of BRAF inhibition and TSH supplementation on ^{131}I uptake of $BRAF^{V600E}$-mutant human thyroid cancer cells.

Materials and methods: WRO cells (a $BRAF^{V600E}$-mutant follicular-derived papillary thyroid carcinoma cell line) were transfected with small interfering RNA targeting BRAF for 72 h in a physiological TSH environment. NIS and TSHr expression were then evaluated at three levels: gene expression, protein levels, and ^{131}I uptake. These three main outcomes were then reassessed in TSH-depleted media and media supplemented with supratherapeutic concentrations of TSH.

Results: NIS gene expression increased 5.5-fold 36 h after transfection ($P = 0.01$), and *TSHr* gene expression increased 2.8-fold at 24 h ($P = 0.02$). NIS and TSHr protein levels were similarly increased 48 and 24 h after transfection, respectively. Seventy-two hours after BRAF inhibition, ^{131}I uptake was unchanged in TSH-depleted media, increased by 7.5-fold ($P < 0.01$) in physiological TSH media, and increased by 9.1-fold ($P < 0.01$) in supratherapeutic TSH media.

Conclusions: The combined strategy of BRAF inhibition and TSH supplementation results in greater ^{131}I uptake than when either technique is used alone. This represents a simple and feasible approach that may improve outcomes in patients with radioactive iodine–resistant thyroid carcinomas for which current treatment algorithms are ineffective.

* *Corresponding author*. Department of Surgery, New York Presbyterian Hospital-Weill Cornell Medical College, 525 E 68th Street, Room F-2024, New York, NY 10065. Tel.: +1 212 746 5130; fax: +1 212 746 9948.
E-mail address: raz2002@med.cornell.edu (R. Zarnegar).

[1] These authors contributed equally to this article.

0022-4804/$ – see front matter © 2013 Elsevier Inc. All rights reserved.
http://dx.doi.org/10.1016/j.jss.2012.08.053

1. Introduction

The loss of radioactive iodine (RAI) uptake in differentiated thyroid carcinomas accounts for significant morbidity and mortality of this increasingly common disease [1,2]. Roughly, 25% of primary well-differentiated thyroid tumors and 50% of metastases are RAI resistant (RAIR), and effective adjuvant medical therapies after thyroidectomy are limited [3].

The efficacy of RAI ablation after thyroidectomy is dependent on active intracellular transport and trapping of iodine by the sodium–iodide symporter (NIS) [4,5]. NIS is a basolateral membrane protein that is regulated by a host of iodine-metabolizing proteins such as the thyroid stimulating hormone receptor (TSHr), which controls transcription and posttranslational modification of NIS [6,7].

A rapidly growing body of literature has implicated members of the mitogen activated protein kinase (MAPK) signaling pathway, of which BRAF is the strongest activator, with tumorigenesis of aggressive thyroid carcinomas [8]. The $BRAF^{V600E}$ mutation is present in 40%–50% of all papillary thyroid cancers (PTC) and is associated with aggressive features, such as extrathyroidal extension, lymph node metastases, advanced tumor stage, and RAIR [9–11]. It is thought that the loss of responsiveness to ^{131}I is because of the loss of function of iodine-metabolizing proteins, such as NIS and TSHr [3,12,13]. Tumor cells harboring this mutation have decreased *NIS* and *TSHr* gene expression compared with similar cells without the mutation [12,14–17]. Several recent *in vitro* and *in vivo* mouse studies have demonstrated that BRAF inhibition with small-molecule MAPK pathway inhibitors restores the expression of iodine-metabolizing proteins and increases susceptibility to RAI [18,19].

It has also been shown that increasing circulating TSH to supratherapeutic levels before treatment with RAI increases its potency [20–22]. It is believed that TSH enhances the function of the NIS and results in increased ^{131}I uptake [7]. For this reason, many centers routinely administer human recombinant TSH or withhold thyroid hormone before ^{131}I therapy to achieve supratherapeutic TSH levels at the time of treatment [22–24].

Thus, it has been independently demonstrated that both BRAF inhibition and TSH supplementation can increase RAI uptake in RAIR tumors; however, the additive potential of implementing both strategies simultaneously has not been reported. We hypothesized that supplementing $BRAF^{V600E}$-mutant human thyroid cancer cells with supratherapeutic concentrations of TSH while transiently inhibiting BRAF would result in greater ^{131}I uptake compared with BRAF inhibition in lower TSH environments.

2. Materials and methods

2.1. Patient selection and analysis

First, to evaluate the prevalence of the $BRAF^{V600E}$ mutation and its effect on tumor behavior and levels of *NIS* and *TSHr*, a representative cohort of patients who underwent surgery for PTC between 2003 and 2010 was selected. After obtaining approval from our institutional review board and written informed consent from each patient, tumor and representative normal tissue samples from the contralateral lobe were collected. All samples were snap frozen in liquid nitrogen and stored at −80°C until analysis. A retrospective review of a prospectively maintained patient database was performed for age, sex, and histopathologic features. All surgical specimens were reviewed by an endocrine pathologist.

2.2. Cell culture

The $BRAF^{V600E}$-mutant human follicular thyroid carcinoma-derived cell line WRO was used in this study. Of note, both $BRAF^{V600E}$-mutant and wild-type WRO cells have been reported, and it is accepted that two distinct cell lines have been distributed [25]. The WRO cells used in this report were confirmed to be the $BRAF^{V600E}$ variety. These cells were a generous gift from Dr James A. Fagin (Memorial Sloan-Kettering, NY) and were validated using short tandem repeat and single-nucleotide polymorphism array analysis in 2008 [25].

2.3. Cell culture media preparation

To investigate the role of TSH in iodine uptake, cells were maintained in three different types of media: H6 (physiological TSH concentration), H5 (no TSH), and supratherapeutic TSH media. H6 medium was made using Hams F-12:Dulbecco's Modified Eagle Medium (DMEM) supplemented with insulin (10 μg/mL), human transferrin (5 μg/mL), somatostatin (1 mg/mL), glycyl-L histidyl-L-lysine acetate (2 ng/mL), hydrocortisone (0.36 ng/mL), TSH (10 mU/mL), penicillin G (100 IU/mL), streptomycin sulfate (100 μg/mL), and amphotericin B (0.25 μg/mL). H5 medium contained the same components as H6 except without TSH. Supratherapeutic TSH media also contained the same components as H6 except for supplementation with 500 mU/mL of TSH. This concentration is similar to that which is achieved after administration of recombinant TSH before RAI ablation.

2.4. Small interfering RNA plasmids and transfection

Two oligonucleotides targeting an area of the *BRAF* gene outside of the V600E mutation site consisting of ribonucleosides with the presence of 2′-deoxyribonucleosides at the 3′-end, 5′-(CGAGACCGAUCCUCAUCAG)d(TT)-3′ and 5′-r(CUG AUGAGGAUCGGUCUCG)d(TT)-3, were synthesized and annealed as previously described (Qiagen, Valencia, CA) [26]. Cells were transfected using Lipofectamine (HiPerFect Transfection Reagent; Qiagen). Transfection experiments were performed using Fast-Forward Transfection protocol according to the manufacturer. A total of 3.5×10^5 cells were seeded into a six-well plate. Cells were exposed to 10, 20, and 40 nmol of small interfering RNA (siRNA) for up to 96 h. Positive controls and transfection efficiency were measured with AllStars Hs Cell Death Control siRNA (Qiagen). Negative control siRNA transfection was performed using a nonsilencing siRNA (AllStars Negative Control siRNA; Qiagen).

2.5. RNA extraction, reverse transcription, and real-time polymerase chain reaction

RNA was extracted from cells and frozen tissue by homogenization in RNeasy Lysis Buffer (Buffer RLT; Qiagen) using the manufacturer's instructions (RNeasy Mini Kit; Qiagen). RNA purity was confirmed by spectrophotometry.

First-strand complementary DNA synthesis was performed using 1 μg of each RNA sample primed with SuperScript First-Strand Synthesis system, Oligo $(dT)^{12-18}$ primer, random hexamers, and superscript II reverse transcriptase (Invitrogen, Carlsbad, CA). A reaction mixture containing 2.5 μL of complementary DNA template, 12.5 μL TaqMan Universal PCR master mix (Applied Biosystems, Foster city, CA), and 1.25 μL primer probe mixture was amplified using the following thermal cycler parameters: incubation at 50°C for 2 min and denaturing at 95°C for 10 min and then 40 cycles of the amplification step (denaturation at 95°C for 15 s and annealing or extension at 60°C for 1 min). *BRAF*, *NIS*, and *TSHr* gene expression were measured in triplicate and normalized relative to the house-keeping gene β-glucoronidase (Applied Biosystems). The mean of the reference-normalized expression measurements (ΔCt) in triplicate was used for statistical analysis. Gene expression values were calculated according to the ΔΔCT method.

2.6. $BRAF^{V600E}$ mutation analysis

Genomic DNA was extracted from cells and tumor samples using the QIAamp DNA Mini Kit (Qiagen) according to the manufacturer's instructions. The following primers adapted from those previously reported [27] were used as a template for a standard polymerase chain reaction (PCR): forward 5′-TGCTTGCTCTGATAGGAAAATG-3′, reverse 5′-GACTTTCTAGTAACTCAGCAGC-3′. The PCR product was purified using the QIAQuick PCR Purification Kit (Qiagen) and visualized on a 2% agarose gel, which confirmed the presence of a single band of approximately 238 bp. The PCR product was then direct sequenced using an Applied Biosystems Automated 3730xl DNA analyzer (Biotechnology Resource Center of Cornell University, Ithaca, NY, USA).

2.7. Western blots

Protein was extracted with radioimmunoprecipitation assay lysis buffer (Santa Cruz Biotechnology, Santa Cruz, CA) containing protease inhibitors. Protein concentration was determined by the Pierce BCA assay method according to the manufacturer's protocol (Thermo Scientific, Waltham, MA).

Fifty micrograms of protein per lane was loaded on a 12% sodium dodecyl sulfate–polyacrylamide gel electrophoresis gel. After a semidry transfer onto nitrocellulose membrane, blots were incubated in a 5% milk in 0.05% Tris buffer saline solution with tween blocking solution for 1 h. Membranes were probed overnight at 4°C with primary antibodies targeting NIS (1:200), TSH (1:1000), or phospho-ERK (P-ERK; 1:200) in 5% milk in 0.05% Tris buffer saline solution with tween (Santa Cruz Biotechnology). Blots were then incubated with horseradish peroxidase–conjugated secondary antibodies (Santa Cruz Biotechnology) as appropriate for 1 h at room temperature. Immunoreactive bands were visualized using Amersham ECL Enhanced Chemiluminescence System (GE Healthcare, Piscataway, NJ). Blots were then stripped with 10 mL of Restore PLUS Western Blot Stripping Buffer (Thermo Scientific, Rockford, IL) and reprobed for either glyceraldehyde 3-phosphate dehydrogenase (GAPDH) (1:10000; Abcam, Cambridge, MA) or β-actin (1:1000; Cell Signaling) as loading controls.

2.8. Radionucleotide uptake in vitro

RAI uptake was measured according to the protocol used by Haddad *et al.* [28] with slight modifications. ^{131}I was measured at 24, 48, 72, and 96 h after siRNA transfection. Cells were trypsonized, and 5×10^5 cells were transferred into each well of a 12-well plate in 1 mL of medium. One mCi of ^{131}I was added to each well and incubated for 30 min. After the completion of incubation time, 0.5 mL of fresh medium was added into each well. Cells were then centrifuged, and the supernatant was transferred into a second test tube at which point the cells were washed with phosphate-buffered saline three times. Tubes were then weighed (#1 containing the pellet of cells, #2 containing media, #3 containing wash 1, and #4 containing wash #2), and the radiation was recorded by a Wizard scintillation well counter. A Pierce BCA protein assay was performed in parallel to measure protein concentration. Results were normalized to protein milligrams and expressed as counts per minute per milligram.

2.9. Statistical analysis

Data was presented as mean ± standard deviation (SD) (normally distributed continuous variables), median, and range (nonnormally distributed continuous variables), % change, or fold-change of gene expression. Significance was assessed using Fisher exact, student *t*-, or Wilcoxon rank sum test as appropriate. Statistical significance was set at $P = 0.05$. Statistical analysis was performed using SPSS 18.0 statistical software (Cornell University, NY).

3. Results

3.1. $BRAF^{V600E}$ mutation and thyroid iodine–metabolizing gene expression in a patient population

A representative cohort of 47 patients who underwent a thyroidectomy for cancer was selected (Table). The $BRAF^{V600E}$ mutation was detected in 24 of the 47 (51%) of the malignant tumors. The presence of extrathyroidal extension was significantly higher (68% *versus* 32%, $P = 0.020$), and the prevalence of the follicular variant of PTC was significantly lower (18.2% *versus* 81.8%, $P = 0.017$) among tumors carrying the $BRAF^{V600E}$ mutation. There was no association between the presence of the $BRAF^{V600E}$ mutation and age, sex, tumor size, lymph node metastases, angiolympathic invasion, and multifocality.

Mean gene expression of *NIS* and *TSHr* was then measured from 10 of the tumors that carried the $BRAF^{V600E}$ mutation and 10 $BRAF^{WT}$ tumors. Tumors carrying the $BRAF^{V600E}$ mutation had significantly lower gene expression of *NIS* (ΔCT ± SD, 0.27 ± 0.03 *versus* 0.78 ± 0.09, $P < 0.01$) and *TSHr* (ΔCT ± SD, 0.42 ± 0.09 *versus* 0.71 ± 0.02, $P < 0.01$) compared with $BRAF^{WT}$ tumors (Table).

Table – Patient demographics, histopathologic features, and iodine-metabolizing gene expression.

Clinical variable	Total (N = 47) (%)	$BRAF^{V600E}$ (N = 24) (%)	$BRAF^{wt}$ (N = 23) (%)	P value*
Patient demographics				
Age (mean ± SD)	44.2 ± 13.9	46.0 ± 15.2	42.2 ± 12.5	0.35
Gender				
Male (N = 12)	12 (25.5)	7 (58.3)	5 (41.7)	0.74
Female (N = 35)	35 (74.5)	17 (48.6)	18 (53.3)	
Histopathologic features				
Tumor size in cm, median (range)	1.5 (0.7–8.0)	1.9 (0.8–8.0)	1.2 (0.7–4.5)	0.12
Histologic subtypes				
PTC	24 (51.1)	13 (54.2)	11 (45.8)	0.77
Follicular variant of PTC	11 (23.4)	2 (18.2)	9 (81.8)	0.02
Tall cell variant of PTC	6 (12.8)	5 (83.3)	1 (16.7)	0.19
Follicular carcinoma	2 (4.3)	0 (0)	2 (100)	0.23
Poorly differentiated	4 (8.5)	4 (100)	0 (0)	0.11
Extrathyroidal extension	25 (53.2)	17 (68)	8 (32)	0.02
Lymphovascular invasion	11 (23.4)	7 (63.4)	4 (36.4)	0.49
Multifocality	18 (38.3)	9 (50.0)	9 (50.0)	1.00
Lymph node metastases	20 (42.6)	11 (55.0)	9 (45.0)	0.77
Iodine-metabolizing gene expression†				
NIS	0.53 ± 0.35	0.27 ± 0.03	0.78 ± 0.09	<0.01
TSHr	0.62 ± 0.05	0.42 ± 0.09	0.71 ± 0.02	<0.01

* *P* values were derived using student *t*-test (age and gene expression), Wilcoxon rank sum test (tumor size), and Fisher exact chi-square (all other variables) test.
† Gene expression was given as ΔΔCT ± SD.

3.2. *Effect of BRAF knockdown in human thyroid cancer cells in a physiological (control) TSH environment*

3.2.1. *Transient knockdown of BRAF in human thyroid cancer cells*

First, to establish the effectiveness of siRNA transfection for inhibiting BRAF and restoring *NIS* and *TSHr* gene expression, transfections were carried out in a physiological (control) TSH environment using three different siRNA doses (10, 20, and 40 nmol). Significant differences in *BRAF*, *NIS*, and *TSHr* gene expression were noted with all three concentrations compared with negative controls, but there were no significant differences among the different concentrations. For simplicity, only the results of the 20 nmol transfections are presented (results of the 10 and 40 nmol transfections are available on request).

BRAF gene expression was decreased by an average of 51% ($P < 0.01$) 24 h after transfection (Fig. 1A). Inhibition was first

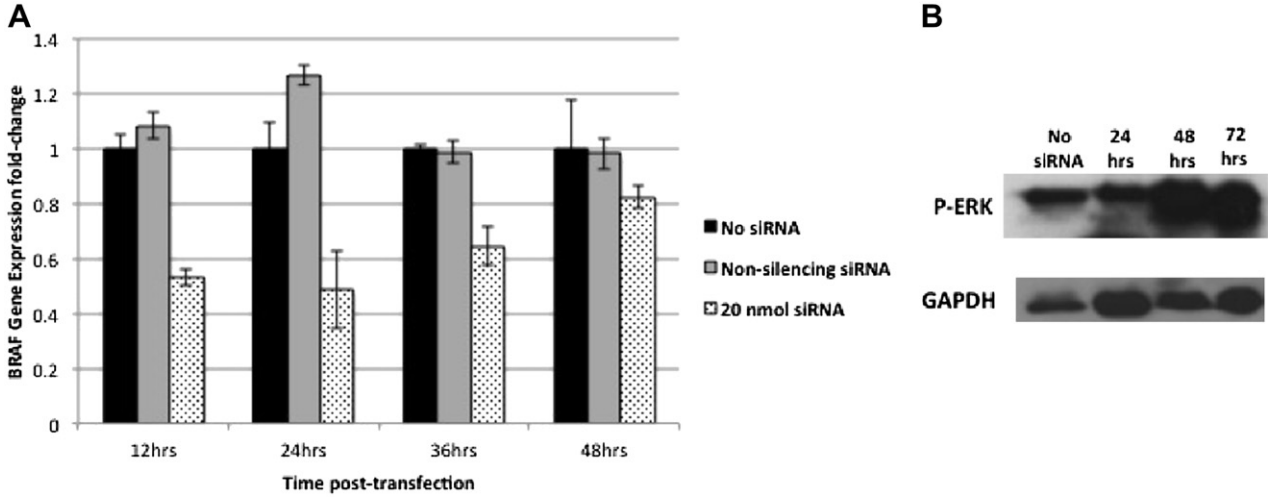

Fig. 1 – Knockdown of BRAF expression after transfection of siRNA in WRO human thyroid cancer cells. (A) Total RNA was quantified by quantitative polymerase chain reaction at four different time points after transfection with 20 nmol of siRNA and compared with nontransfected cells and transfection with nonsilencing siRNA. WRO cells exhibited a 51% ($P < 0.01$) decrease in *BRAF* gene expression 24 h after transfection. This inhibitory effect was first observed at 12 h and returned to near-baseline by 48 h. (B) Western blot of P-ERK (a downstream actuator of the RAF/MEK/ERK signal pathway) showing a 27% reduction of protein levels when normalized to glyceraldehyde 3-phosphate dehydrogenase (GAPDH) 24 h after transfection and recovery of pretransfection levels by 48 h.

detected at 12 h and returned to near-baseline levels at 36 h. To measure *BRAF* activity at the protein level, Western blots for P-ERK (the main downstream actuator of the MAP/MEK/ERK cascade) were performed at baseline, 24, 48, and 72 h after siRNA transfection. A transient 27% decrease in P-ERK protein expression occurred at 24 h and returned to slightly above baseline by 72 h (Fig. 1B).

3.2.2. *Restoration of NIS and TSHr gene expression and protein levels after siRNA transfection*

To evaluate the effect of BRAF inhibition on iodine-metabolizing proteins, NIS and TSHr gene expression and protein levels were measured pre- and posttransfection. *NIS* gene expression increased by an average of 3.9-fold ($P = 0.01$) 36 h after siRNA transfection relative to nontransfected cells and returned to near-baseline by 48 h (Fig. 2A). NIS Western blots performed at 24, 48, and 72 h after transfection revealed a band at 50 kDa (nonglycosylated NIS) and an additional wide band of approximately 87–150 kDa (glycosylated NIS), as has been described previously [29]. NIS protein levels increased by 50% 48 h and returned to baseline by 72 h (Fig. 2B).

TSHr gene expression increased by an average of 2.5-fold ($P = 0.02$) 24 h after transfection (Fig. 2C). TSHr protein levels similarly increased at 24 h compared with pretransfection levels and returned to baseline by 48 h (Fig. 2D).

3.3. *Effect of TSH withdrawal and supplementation on iodine uptake after BRAF inhibition*

3.3.1. *Effect of TSH withdrawal on iodine-metabolizing genes*

WRO cells grown in H5 media (no TSH) were found to have significantly lower *NIS* gene expression 36 h after transfection than those grown in H6 media (physiological TSH concentration) (ΔCT ± SD, 2.6 ± 0.02 *versus* 4.7 ± 0.07, $P = 0.02$) (Fig. 3A).

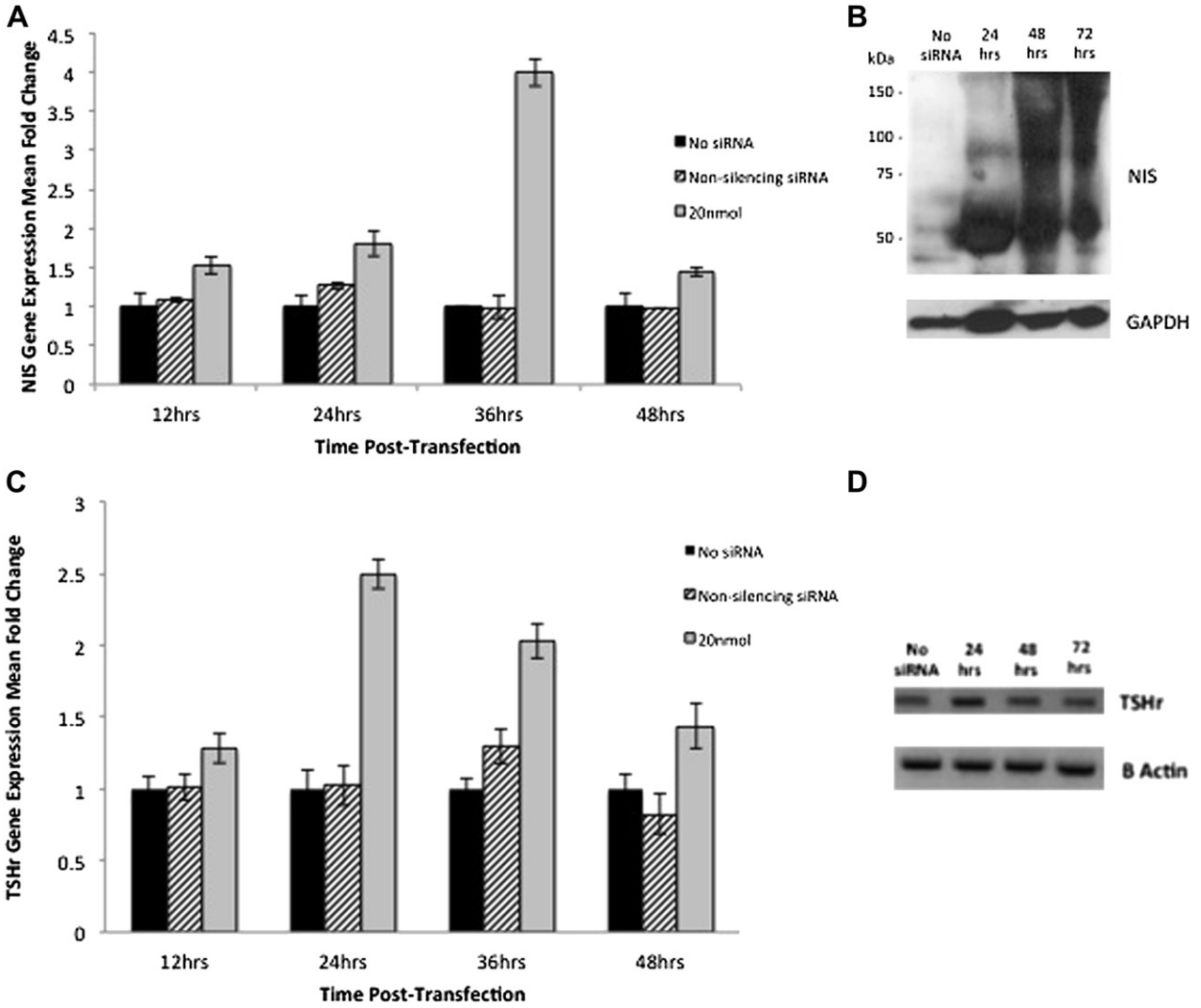

Fig. 2 – Changes in NIS and TSHr gene expression and protein levels after transfection of 20 nmol of siRNA in WRO cells compared with nontransfected cells and transfection with nonsilencing siRNA in a physiological (control) TSH environment. (A) *NIS* gene expression increased by 3.9-fold ($P = 0.01$) 36 h after transfection with 20 nmol of siRNA. (B) Western blot of NIS showing a 50% increase of protein levels 48 h after transfection that returned to baseline by 72 h. (C) *TSHr* gene expression increased by 2.5-fold ($P = 0.02$) 24 h after transfection with 20 nmol of siRNA. (D) Western blot of TSHr showing increased protein levels at 24 h after transfection that returned to baseline by 48 h.

Similarly, *TSHr* gene expression was significantly lower in cells grown in H5 media compared with those grown in H6 media 24 h after transfection in WRO (ΔCT ± SD, 1.4 ± 0.01 *versus* 2.2 ± 0.07, $P = 0.03$) (Fig. 3B).

3.3.2. *Effect of TSH concentration on ^{131}I uptake after BRAF inhibition*

TSH concentration was found to have a significant dose-dependent effect on ^{131}I uptake after siRNA transfection (Fig. 4). WRO cells grown in H5 media (no TSH) showed no increase in ^{131}I uptake 72 h after siRNA transfection compared with nontransfected cells, whereas WRO cells grown in H6 media (physiological TSH) showed a 7.5-fold ($P < 0.01$) increase at the same time point. Furthermore, supplementing the media with supratherapeutic TSH resulted in an even greater 9.1-fold increase of ^{131}I uptake ($P < 0.01$) at 72 h compared with nontransfected cells. The maximal ^{131}I uptake that was achieved in the supratherapeutic TSH environment was 1.7-fold higher than that achieved in physiological TSH conditions ($P < 0.01$). ^{131}I uptake was not significantly changed when cells grown in any of the three conditions were not transfected or were transfected with nonsilencing siRNA (Fig. 4).

4. Discussion

RAIR thyroid cancers present a deadly dilemma for patients and clinicians, as currently alternate medical treatments for local recurrences and metastases are limited [24]. Because the $BRAF^{V600E}$ mutation is present in most RAIR tumors, it is an

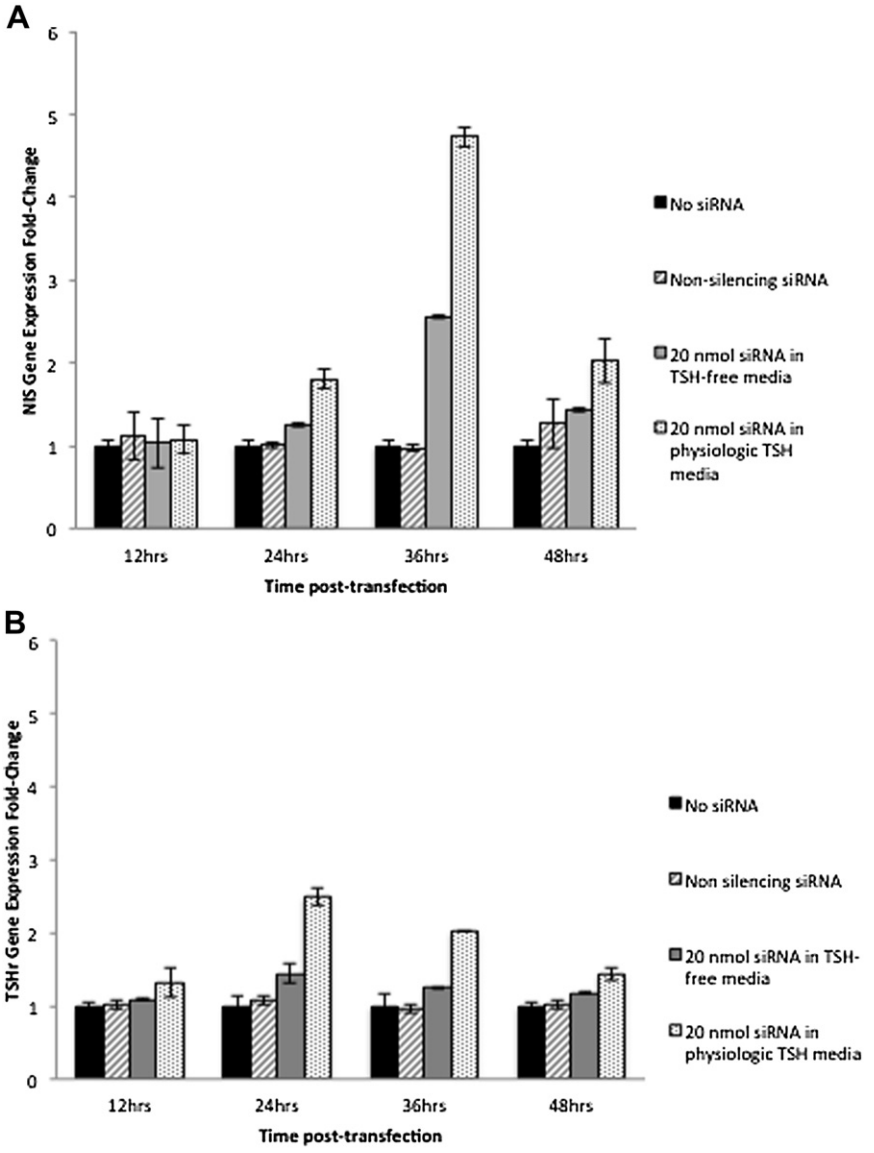

Fig. 3 – The effect of ambient TSH on *NIS* and *TSHr* gene expression after BRAF silencing. (A) WRO cells grown in H6 media (physiological TSH concentration) were found to have significantly increased *NIS* recovery 36 h after transfection with siRNA compared with those grown in H5 (TSH-free) media (4.7 ± 0.07 *versus* 2.6 ± 0.02, $P = 0.02$). (B) *TSHr* gene expression recovery was also significantly higher in cells grown in H6 media compared with those grown in H5 media 24 h after transfection in WRO cells (2.2 ± 0.07 *versus* 1.4 ± 0.01, $P = 0.03$).

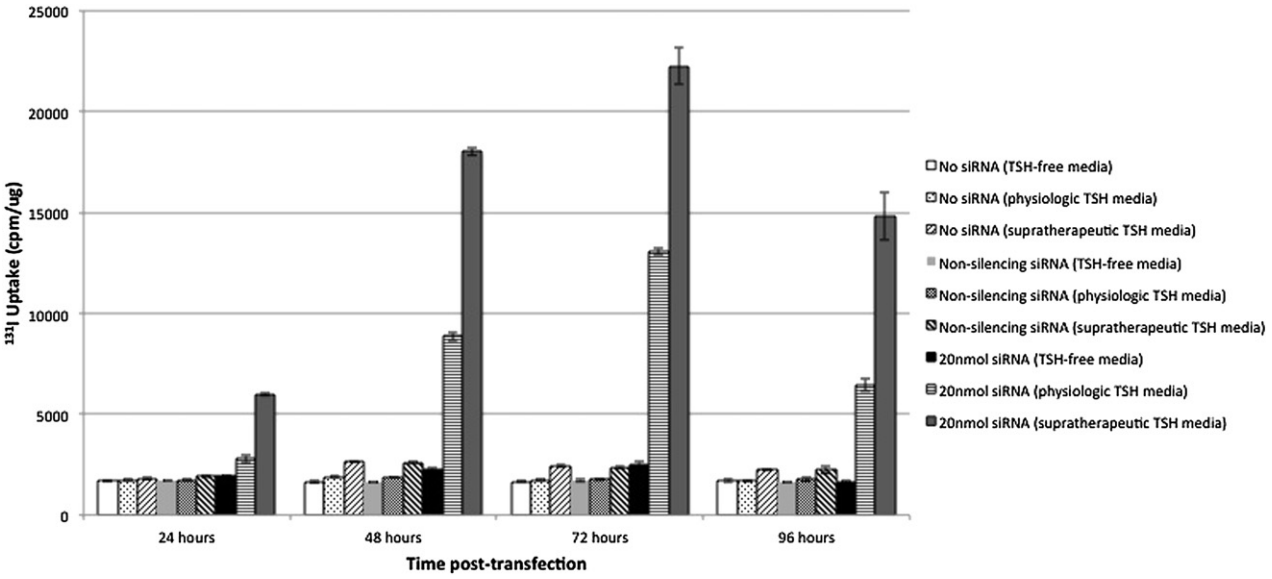

Fig. 4 – ^{131}I uptake of WRO cells after transfection of 20 nmol of siRNA^{BRAF} when grown in three different TSH environments: no TSH (H5), physiological TSH (H6), and media supplemented with ×50 the physiological concentration of TSH (supratherapeutic). ^{131}I uptake did not increase in TSH-free media, increased by 7.5-fold ($P < 0.01$) in physiological TSH media, and increased by 9.1-fold ($P < 0.01$) in supratherapeutic TSH media 72 h after siRNA transfection. Nontransfected WRO cells and WRO cells transfected with nonsilencing siRNA grown in all three media conditions are shown as negative controls.

attractive candidate for the development of targeted molecular therapies.

In the first part of this study, we demonstrated in a small representative patient population that the BRAF^{V600E} mutation is associated with aggressive clinical features and decreased expression of *NIS* and *TSHr*. Both these observations have been reported previously [30–34] and are included to provide a clinical context for the subsequent *in vitro* data.

The main aim of this study was to determine if the combination of *BRAF* inhibition and TSH supplementation results in greater cellular iodine uptake than implementation of each strategy independently. This multimodal approach uses two strategies that already have been established or are currently under clinical investigation independently and thus offers a simple and feasible strategy to restore susceptibility of RAIR tumors to ^{131}I. To inhibit *BRAF*, we elected to use siRNA against the *BRAF* gene because of the highly specific inhibition of *BRAF* that is achieved. The same specificity is not achieved with similar strategies that use tyrosine kinase inhibitors or small molecules MAPK pathway inhibitors such as PLX4720.

To quantify the activity of the RAF/MEK/ERK pathway at the protein level after *BRAF* inhibition, we elected to measure P-ERK levels rather than BRAF. P-ERK lies downstream of BRAF and activates hundreds of other transcription factors during activation of the cascade [35,36]. Therefore, measuring this step of the pathway provides the most direct assessment of its overall activity. In addition, Western blots for P-ERK are more reliable and more reproducible than those for BRAF, and therefore, P-ERK is more suitable for use in this study. Although a profound inhibitory effect on BRAF and P-ERK was not observed with siRNA transfection, the inefficiency of knockdown of this pathway has previously been reported. Galabova–Kovacs *et al.* [37] demonstrated that knocking out *BRAF* in mouse embryos resulted in virtual absence of P-ERK in the placenta but only a 60% reduction in the embryo. Pritcherd *et al.* [38] similarly observed an incomplete reduction of P-ERK levels in fibroblasts of *BRAF*-knockout mice. These findings have led to the conclusion that a complex array of cell signaling and kinase activity occurs along multiple steps of the RAF/MEK/ERK pathway that can circumvent BRAF-dependent kinase activity [39]. Thus, targeting a single step along this pathway in an attempt to abrogate downstream activity has proven to be a difficult and often inefficient endeavor.

Increasing expression of iodine-metabolizing genes by knocking down BRAF is not, by itself, a novel concept. In 2007, Liu *et al.* [40] observed restoration of *TSHr* and *NIS* gene expression in BRAF^{V600E}-mutant human PTC cells after transfection with U0126, a direct MEK pathway inhibitor. More recently, Chakravarty *et al.* [18] demonstrated in mice engineered with doxycycline-inducible BRAF^{V600E} expression that the activation of the BRAF mutation results in near-complete abolition of several iodine-metabolizing genes including *NIS* and *TSHr*. The expression of these genes and ^{124}I thyroid uptake were partially recovered by switching off the BRAF^{V600E} mutation and also by treating the mice with PLX4720, a small molecule BRAF inhibitor. Interestingly, dox induction of BRAF^{V600E} also rendered the mice hypothyroid and significantly increased plasma TSH concentrations at the time of the iodine uptake assays. Although the mice returned to a euthyroid state 2 wk after doxycycline withdrawal, iodine uptake was not reassessed at that time, and

therefore, the influence of the elevated TSH is unclear from this study.

There are two main limitations to this article. First, the siRNA used in this study targets a region of the BRAF gene outside of the V600E mutation site and thus silences BRAF wild-type and mutant cells equally. It is therefore unclear that if these results are unique to $BRAF^{V600E}$ mutants or could be observed in BRAF wild-type cells as well. Second, the effect of the siRNA transfection on BRAF gene expression was modest, and the observed changes at the protein level were even smaller. As noted previously, the intricacies of the RAF/MEK/ERK pathway are not yet completely understood, and it is believed that multiple escape pathways exist involving other members of the RAF family of kinases to continue MEK and ERK phosphorylation despite BRAF inhibition.

In conclusion, we have demonstrated that the simultaneous implementation of two independent treatment strategies for RAIR thyroid tumors (BRAF inhibition and TSH supplementation) increases ^{131}I uptake more effectively than when either modality is implemented alone. This promising approach represents a substantial advancement in the treatment of RAIR thyroid cancers and may offer a new option for patients who have failed our current treatment algorithms.

Acknowledgment

This investigation was supported in part by grant TL1RR024998 of the Clinical and Translational Science Center at Weill Cornell Medical College and by the Dancers Care Foundation.

REFERENCES

[1] Durante C, Haddy N, Baudin E, et al. Long-term outcome of 444 patients with distant metastases from papillary and follicular thyroid carcinoma: benefits and limits of radioiodine therapy. J Clin Endocrinol Metab 2006;91:2892.
[2] Antonelli A, Fallahi P, Ferrari SM, et al. Dedifferentiated thyroid cancer: a therapeutic challenge. Biomed Pharmacother 2008;62:559.
[3] Zarnegar R, Brunaud L, Kanauchi H, et al. Increasing the effectiveness of radioactive iodine therapy in the treatment of thyroid cancer using Trichostatin A, a histone deacetylase inhibitor. Surgery 2002;132:984. discussion 990.
[4] Riesco-Eizaguirre G, Santisteban P. A perspective view of sodium iodide symporter research and its clinical implications. Eur J Endocrinol 2006;155:495.
[5] Nilsson M. Iodide handling by the thyroid epithelial cell. Exp Clin Endocrinol Diabetes 2001;109:13.
[6] Dai G, Levy O, Carrasco N. Cloning and characterization of the thyroid iodide transporter. Nature 1996;379:458.
[7] Saito T, Endo T, Kawaguchi A, et al. Increased expression of the Na+/I-symporter in cultured human thyroid cells exposed to thyrotropin and in Graves' thyroid tissue. J Clin Endocrinol Metab 1997;82:3331.
[8] Davies H, Bignell GR, Cox C, et al. Mutations of the BRAF gene in human cancer. Nature 2002;417:949.
[9] Lee JH, Lee ES, Kim YS. Clinicopathologic significance of BRAF V600E mutation in papillary carcinomas of the thyroid: a meta-analysis. Cancer 2007;110:38.
[10] Michaloglou C, Vredeveld LC, Mooi WJ, Peeper DS. BRAF(E600) in benign and malignant human tumours. Oncogene 2008;27:877.
[11] Kim TH, Park YJ, Lim JA, et al. The association of the BRAF(V600E) mutation with prognostic factors and poor clinical outcome in papillary thyroid cancer: a meta-analysis. Cancer 2012 Apr 1;118(7):1764.
[12] Riesco-Eizaguirre G, Rodriguez I, De la Vieja A, et al. The BRAFV600E oncogene induces transforming growth factor beta secretion leading to sodium iodide symporter repression and increased malignancy in thyroid cancer. Cancer Res 2009;69:8317.
[13] Ricarte-Filho JC, Ryder M, Chitale DA, et al. Mutational profile of advanced primary and metastatic radioactive iodine-refractory thyroid cancers reveals distinct pathogenetic roles for BRAF, PIK3CA, and AKT1. Cancer Res 2009;69:4885.
[14] Durante C, Puxeddu E, Ferretti E, et al. BRAF mutations in papillary thyroid carcinomas inhibit genes involved in iodine metabolism. J Clin Endocrinol Metab 2007;92:2840.
[15] Espadinha C, Santos JR, Sobrinho LG, Bugalho MJ. Expression of iodine metabolism genes in human thyroid tissues: evidence for age and BRAFV600E mutation dependency. Clin Endocrinol (Oxf) 2009;70:629.
[16] Oler G, Cerutti JM. High prevalence of BRAF mutation in a Brazilian cohort of patients with sporadic papillary thyroid carcinomas: correlation with more aggressive phenotype and decreased expression of iodide-metabolizing genes. Cancer 2009;115:972.
[17] Romei C, Ciampi R, Faviana P, et al. BRAFV600E mutation, but not RET/PTC rearrangements, is correlated with a lower expression of both thyroperoxidase and sodium iodide symporter genes in papillary thyroid cancer. Endocr Relat Cancer 2008;15:511.
[18] Chakravarty D, Santos E, Ryder M, et al. Small-molecule MAPK inhibitors restore radioiodine incorporation in mouse thyroid cancers with conditional BRAF activation. J Clin Invest 2011;121:4700.
[19] Nucera C, Nehs MA, Nagarkatti SS, et al. Targeting BRAFV600E with PLX4720 displays potent antimigratory and anti-invasive activity in preclinical models of human thyroid cancer. Oncologist 2011;16:296.
[20] Pacini F, Ladenson PW, Schlumberger M, et al. Radioiodine ablation of thyroid remnants after preparation with recombinant human thyrotropin in differentiated thyroid carcinoma: results of an international, randomized, controlled study. J Clin Endocrinol Metab 2006;91:926.
[21] Pilli T, Brianzoni E, Capoccetti F, et al. A comparison of 1850 (50 mCi) and 3700 MBq (100 mCi) 131-iodine administered doses for recombinant thyrotropin-stimulated postoperative thyroid remnant ablation in differentiated thyroid cancer. J Clin Endocrinol Metab 2007;92:3542.
[22] Cooper DS, Doherty GM, Haugen BR, et al. Revised American Thyroid Association management guidelines for patients with thyroid nodules and differentiated thyroid cancer. Thyroid 2009;19:1167.
[23] Ma C, Xie J, Liu W, et al. Recombinant human thyrotropin (rhTSH) aided radioiodine treatment for residual or metastatic differentiated thyroid cancer. Cochrane Database Syst Rev; 2010:CD008302.
[24] O'Neill CJ, Oucharek J, Learoyd D, Sidhu SB. Standard and emerging therapies for metastatic differentiated thyroid cancer. Oncologist 2010;15:146.
[25] Schweppe RE, Klopper JP, Korch C, et al. Deoxyribonucleic acid profiling analysis of 40 human thyroid cancer cell lines reveals cross-contamination resulting in cell line

redundancy and misidentification. J Clin Endocrinol Metab 2008;93:4331.
[26] Mitsiades CS, Negri J, McMullan C, et al. Targeting BRAFV600E in thyroid carcinoma: therapeutic implications. Mol Cancer Ther 2007;6:1070.
[27] Arora N, Scognamiglio T, Lubitz CC, et al. Identification of borderline thyroid tumors by gene expression array analysis. Cancer 2009;115:5421.
[28] Haddad D, Chen NG, Zhang Q, et al. Insertion of the human sodium iodide symporter to facilitate deep tissue imaging does not alter oncolytic or replication capability of a novel vaccinia virus. J Transl Med 2011;9:36.
[29] Levy O, Dai G, Riedel C, et al. Characterization of the thyroid Na+/I-symporter with an anti-COOH terminus antibody. Proc Natl Acad Sci U S A 1997;94:5568.
[30] Kimura ET, Nikiforova MN, Zhu Z, et al. High prevalence of BRAF mutations in thyroid cancer: genetic evidence for constitutive activation of the RET/PTC-RAS-BRAF signaling pathway in papillary thyroid carcinoma. Cancer res 2003; 63:1454.
[31] Xing M. BRAF mutation in papillary thyroid cancer: pathogenic role, molecular bases, and clinical implications. Endocr Rev 2007;28:742.
[32] Jin L, Sebo TJ, Nakamura N, et al. BRAF mutation analysis in fine needle aspiration (FNA) cytology of the thyroid. Diagn Mol Pathol 2006;15:136.
[33] Kim J, Giuliano AE, Turner RR, et al. Lymphatic mapping establishes the role of BRAF gene mutation in papillary thyroid carcinoma. Ann Surg 2006;244:799.
[34] Kim KH, Kang DW, Kim SH, et al. Mutations of the BRAF gene in papillary thyroid carcinoma in a Korean population. Yonsei Med J 2004;45:818.
[35] Yoon S, Seger R. The extracellular signal-regulated kinase: multiple substrates regulate diverse cellular functions. Growth factors 2006;24:21.
[36] Roberts PJ, Der CJ. Targeting the Raf-MEK-ERK mitogen-activated protein kinase cascade for the treatment of cancer. Oncogene 2007;26:3291.
[37] Galabova-Kovacs G, Matzen D, Piazzolla D, et al. Essential role of B-Raf in ERK activation during extraembryonic development. Proc Natl Acad Sci U S A 2006;103:1325.
[38] Pritchard CA, Hayes L, Wojnowski L, et al. B-Raf acts via the ROCKII/LIMK/cofilin pathway to maintain actin stress fibers in fibroblasts. Mol Cell Biol 2004;24:5937.
[39] Galabova-Kovacs G, Kolbus A, Matzen D, et al. ERK and beyond: insights from B-Raf and Raf-1 conditional knockouts. Cell cycle 2006;5:1514.
[40] Liu D, Hu S, Hou P, et al. Suppression of BRAF/MEK/MAP kinase pathway restores expression of iodide-metabolizing genes in thyroid cells expressing the V600E BRAF mutant. Clin Cancer Res 2007;13:1341.